

The ANTARES neutrino telescope

Juan de Dios Zornoza¹ and Juan Zúñiga¹

on behalf of the ANTARES collaboration

¹ IFIC, Instituto de Física Corpuscular (CSIC-Universitat de València), Ed. Institutos de Investigación de Paterna, AC22085, 46071 Valencia, Spain

Abstract

The ANTARES collaboration completed the installation of the first neutrino detector in the sea in 2008. It consists of a three dimensional array of 885 photomultipliers to gather the Cherenkov photons induced by relativistic muons produced in charged-current interactions of high energy neutrinos close to/in the detector. The scientific scope of neutrino telescopes is very broad: the origin of cosmic rays, the origin of the TeV photons observed in many astrophysical sources or the nature of dark matter. The data collected up to now have allowed us to produce a rich output of physics results, including the map of the neutrino sky of the Southern hemisphere, search for correlations with GRBs, flaring sources, gravitational waves, limits on the flux produced by dark matter self-annihilations, etc. In this paper a review of these results is presented.

1 Introduction

Neutrino astronomy is a powerful tool both for the astrophysics and the particle physics fields. Neutrinos have specific advantages to study the Universe compared to other more traditional probes, like photons or cosmic rays. Photons, in particular at high energies, are absorbed by matter and radiation, which severely limits their range in the >1 TeV region. Cosmic rays (CRs) also interact with matter and radiation and in addition to this, they are deflected by galactic and extra-galactic magnetic fields. Neutrinos, on the other hand, are neutral and only interact weakly, which makes them unique sources of information of the high energy Universe. The price to pay, given that they only interact weakly and that the expected fluxes are low, is that large detection volumes are needed.

The scientific scope for neutrino telescopes is very wide. One of the main goals is to understand the origin of CRs. A century has past since V. Hess showed that they are produced outside the Earth. Since they are deflected by magnetic fields, as mentioned above, it is not clear which sources are producing them, in particular for high energies. However, in the interactions of high energy CRs mentioned above, high energy neutrinos are also produced:

$$\begin{aligned}
N + X \longrightarrow \pi^\pm(K^\pm \dots) + Y \longrightarrow \mu^\pm + \nu_\mu(\bar{\nu}_\mu) + Y \\
\downarrow \\
e^\pm + \bar{\nu}_\mu(\nu_\mu) + \nu_e(\bar{\nu}_e)
\end{aligned}
\tag{1}$$

Therefore, the observation of neutrinos, which are neutral and therefore not deflected, can help to pinpoint the sources producing CRs [13, 11, 16].

Another important question that neutrino telescopes can help to solve concerns the origin of the high energy photons observed in many astrophysical sources. There are two basic mechanisms through which these photons can be produced. One is based on the so-called leptonic scenarios, in which the photons are produced via processes like inverse Compton scattering. In some of the sources, this mechanism can explain well the observations. However, this is not the case in many sources, like supernova remnant RX1713.7 3946 [12]. In these cases, hadronic mechanisms can be invoked in which the observed high energy gammas are due to the decay of neutral pions produced in the interactions of nucleons with matter or radiation. These neutral pions will decay and produce high energy photons. Therefore, the observation of neutrinos from the decay of charged pions also produced in these interactions would support the hadronic scenarios.

The structure of the paper is as follows. The detection principle and the ANTARES neutrino detector will be described in Section 2. Section 3 presents the results of the search for steady point sources. The studies made on transient sources are explained in Section 4. The search for diffuse cosmic fluxes are described in Section 5. The analysis looking for dark matter is presented in Section 6. Section 7 summarizes other searches performed by the Collaboration. Finally, the conclusions are presented in Section 8.

2 The ANTARES telescope

The detection principle of neutrino telescopes is as follows. The detector is a three-dimensional array of photomultiplier tubes (PMTs) which collect the Cherenkov light induced by relativistic muons produced in the charged-current interactions of high energy muon neutrinos in the surroundings of the detector. Other signatures are also possible: cascade events produced in the neutral current interactions of all the neutrino flavors or in the charged-current interactions of electron and tau neutrinos.

ANTARES [10] is installed in the Mediterranean Sea at a depth of 2475 m and at about 40 km from Toulon (France). It is made of 885 PMTs distributed along 12 mooring lines anchored in the bottom of the sea. The PMTs are enclosed in glass spheres (OMs). The OMs are grouped in triplets, being the separation between triplets (or floors) 14.5 m. The separation between lines is 60-75 m. The lines are connected to a "junction-box" which is linked to the shore station through an electro-optical cable. A system of hydrophones and compasses installed in the detector keeps track of the line movements, allowing for a

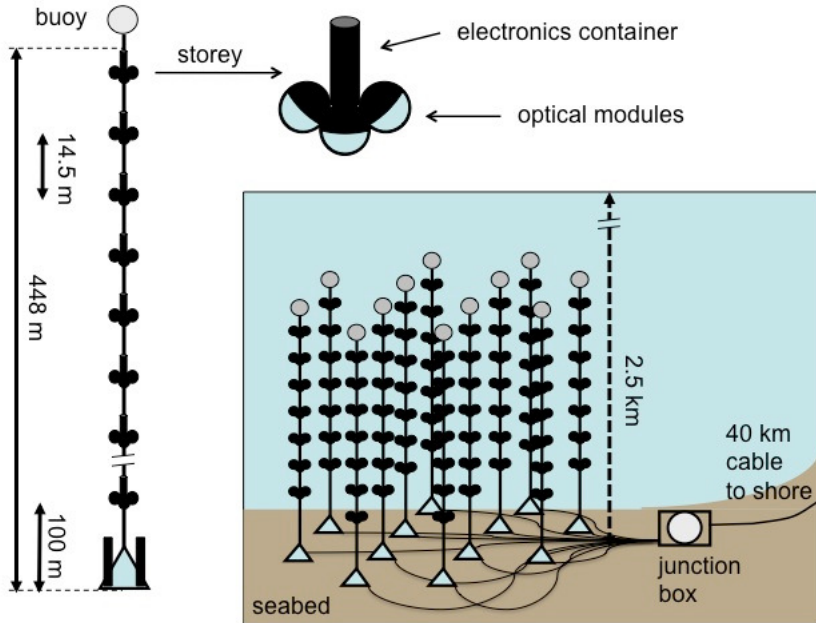


Figure 1 Schematic view of the ANTARES neutrino telescope. It contains 885 PMTs distributed along 12 lines anchored at the sea bottom.

resolution of about 15 cm in the position of the line elements [4]. In order to achieve sub-degree angular resolution, it is also important the time calibration [8] of the detector. This is done by several complementary systems, like the set of LED-based devices called Optical Beacons. A schematic view of the detector is shown in Figure 1.

3 Point source search

The search for cosmic point sources is one of the main goals of neutrino telescopes. The basic strategy for this analysis is to look for an accumulation of events in the sky, so that the probability that the background (atmospheric neutrinos and muons) has produced it by chance is very low. We also use the fact that the energy spectrum for cosmic signal is harder than for the background, so the typical energy for signal events is higher. The cluster search is made by means of a likelihood procedure. The background is estimated directly from data (by randomizing the events in right ascension) in order to reduce systematic effects. For the signal, Monte Carlo simulations provide the point-spread function, which depends on the energy of the event. A first analysis was done with data of 2007-2008 [1]. For the analysis presented here, data from 29-1-2007 to 14-11-2010 are used [7]. The integrated live-time is 813 days, out of which 183 correspond to the period when only five lines were installed.

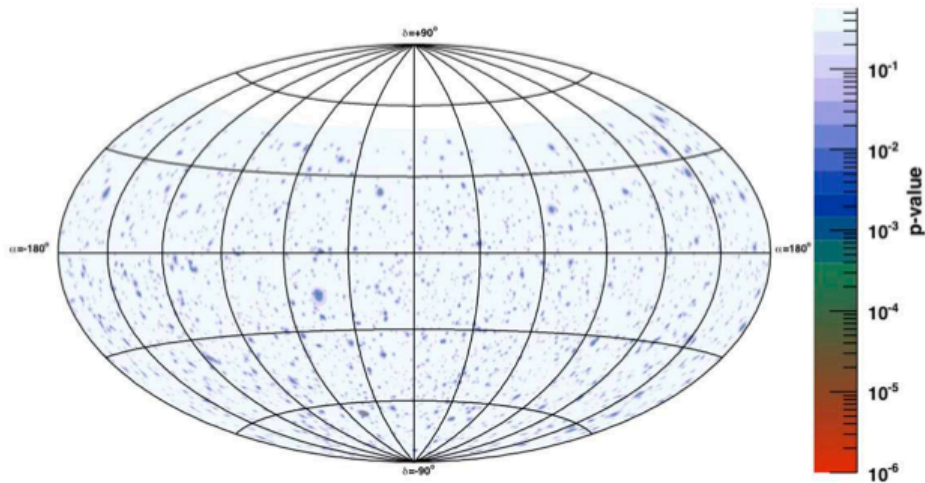


Figure 2 Skymap in equatorial coordinates of p-values obtained in the all-sky search. The trial factor correction is not included in the values shown in the figure. (Preliminary).

The selection of the events is based on several criteria. First, only up-going events are selected. This condition rejects most of the atmospheric muon background, since muons cannot traverse the Earth. This is not enough to reject the atmospheric muon background at an acceptable level, since a fraction of them (small, but given the fact that the flux is very large, not negligible) are mis-reconstructed as up-going events. However, the quality of the fit for these misreconstructed events is bad, so a parameter describing such reconstruction quality is used to further reject this background. Finally, the estimated error in the reconstructed track direction is required to be $< 1^\circ$. The final sample contains 3058 neutrino candidates. Simulations predict 358 ± 179 atmospheric muons and 2040 ± 722 atmospheric neutrinos, consistent with observation. The angular resolution for this sample, assuming an E^{-2} spectrum, is estimated in 0.46 ± 0.10 degrees.

Two different strategies have been followed for this analysis. First, an all-sky search, where the whole sky is scanned looking for accumulations of events. Figure 2 shows the sky map of the p-values before trial factor corrections. The most signal-like cluster is found in $(\alpha, \delta) = (-46.5^\circ, -65.0^\circ)$, where there are five events within one degree around this position. By generating pseudo-experiments for the only-background assumption, it is estimated that the post-trial p-values is 2.6%, equivalent to 2.2σ significance (two-sided sigma convention). Secondly, a search in the direction of 51 sources which are good candidates for neutrino emission. No excess has been found in any of these searches (see Table 1), being the most significant cluster found in HESS J1023-575, with a p-value of 0.41. Upper limits in the neutrino flux are set, as shown in Fig. 3.

Table 1. Results from the search in the candidate list. The equatorial coordinates (α_s, δ_s) in degrees, $1-p$ -value (p) probability and the 90% C.L. upper limit on the E_ν^{-2} flux intensity $\phi^{90\%CL}$ in units of $10^{-8}\text{GeV}^{-1}\text{cm}^{-2}\text{s}^{-1}$ are given (sorted in order of decreasing $1-p$ -value) for the 51 selected sources.

| Source name | α_s [°] | δ_s [°] | $1-p$ | $\phi^{90\%CL}$ | Source name | α_s [°] | δ_s [°] | $1-p$ | $\phi^{90\%CL}$ |
|-----------------|----------------|----------------|-----------|-----------------|-----------------|----------------|----------------|-----------|-----------------|
| HESS J1023-575 | 155.83 | -57.76 | 0.5874970 | 6.6 | SS 433 | -72.04 | 4.98 | 0.0009264 | 4.6 |
| 3C 279 | -165.95 | -5.79 | 0.5231861 | 10.1 | HESS J1614-518 | -116.42 | -51.82 | 0.0009264 | 2.0 |
| GX 339-4 | -104.30 | -48.79 | 0.2775692 | 5.8 | RX J1713.7-3946 | -101.75 | -39.75 | 0.0009264 | 2.7 |
| Cir X-1 | -129.83 | -57.17 | 0.2135361 | 5.8 | 3C454.3 | -16.50 | 16.15 | 0.0009264 | 5.5 |
| MGRO J1908+06 | -73.01 | 6.27 | 0.1803912 | 10.1 | W28 | -89.57 | -23.34 | 0.0009264 | 3.4 |
| ESO 139-G12 | -95.59 | -59.94 | 0.0607835 | 5.4 | HESS J0632+057 | 98.24 | 5.81 | 0.0009263 | 4.6 |
| HESS J1356-645 | -151.00 | -64.50 | 0.0229395 | 5.1 | PKS 2155-304 | -30.28 | -30.22 | 0.0009263 | 2.7 |
| PKS 0548-322 | 87.67 | -32.27 | 0.0146601 | 7.1 | HESS J1741-302 | -94.75 | -30.20 | 0.0009262 | 2.7 |
| HESS J1837-069 | -80.59 | -6.95 | 0.0088167 | 8.0 | Centaurus A | -158.64 | -43.02 | 0.0009263 | 2.1 |
| PKS 0454-234 | 74.27 | -23.43 | 0.0015054 | 7.0 | RX J0852.0-4622 | 133.00 | -46.37 | 0.0009262 | 1.5 |
| IC40 hotspot | 75.45 | -18.15 | 0.0011516 | 7.0 | 1ES 1101-232 | 165.91 | -23.49 | 0.0009262 | 2.8 |
| PKS 1454-354 | -135.64 | -35.67 | 0.0009289 | 5.0 | Vela X | 128.75 | -45.60 | 0.0009262 | 1.5 |
| RGB J0152+017 | 28.17 | 1.79 | 0.0009276 | 6.3 | W51C | -69.25 | 14.19 | 0.0009262 | 3.6 |
| Geminga | 98.31 | 17.01 | 0.0009273 | 7.3 | PKS 0426-380 | 67.17 | -37.93 | 0.0009262 | 1.4 |
| PSR B1259-63 | -164.30 | -63.83 | 0.0009270 | 3.0 | LS 5039 | -83.44 | -14.83 | 0.0009262 | 2.7 |
| PKS 2005-489 | -57.63 | -48.82 | 0.0009269 | 2.8 | W44 | -75.96 | 1.38 | 0.0009262 | 3.1 |
| HESS J1616-508 | -116.03 | -50.97 | 0.0009268 | 2.7 | RCW 86 | -139.32 | -62.48 | 0.0009262 | 1.1 |
| HESS J1503-582 | -133.54 | -58.74 | 0.0009268 | 2.8 | Crab | 83.63 | 22.01 | 0.0009262 | 4.1 |
| HESS J1632-478 | -111.96 | -47.82 | 0.0009267 | 2.6 | HESS J1507-622 | -133.28 | -62.34 | 0.0009261 | 1.1 |
| H 2356-309 | -0.22 | -30.63 | 0.0009266 | 3.9 | 1ES 0347-121 | 57.35 | -11.99 | 0.0009261 | 1.9 |
| MSH 15-52 | -131.47 | -59.16 | 0.0009266 | 2.6 | VER J0648+152 | 102.20 | 15.27 | 0.0009261 | 2.8 |
| Galactic Centre | -93.58 | -29.01 | 0.0009266 | 3.8 | PKS 0537-441 | 84.71 | -44.08 | 0.0009261 | 1.3 |
| HESS J1303-631 | -164.23 | -63.20 | 0.0009265 | 2.4 | HESS J1912+101 | -71.79 | 10.15 | 0.0009261 | 2.5 |
| HESS J1834-087 | -81.31 | -8.76 | 0.0009265 | 4.3 | PKS 0235+164 | 39.66 | 16.61 | 0.0009261 | 2.8 |
| PKS 1502+106 | -133.90 | 10.52 | 0.0009265 | 5.2 | IC443 | 94.21 | 22.51 | 0.0009261 | 2.8 |
| | | | | | PKS 0727-11 | 112.58 | 11.70 | 0.0009261 | 1.9 |

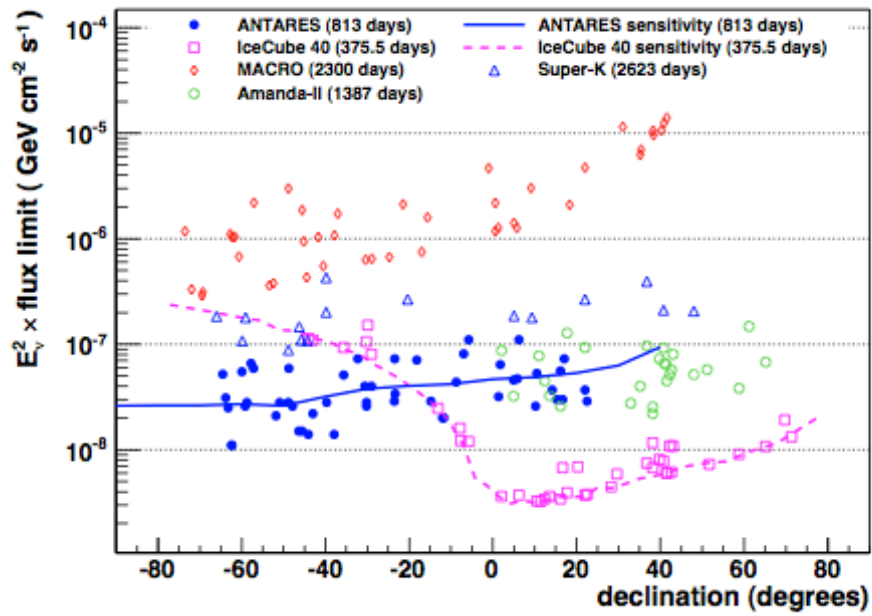


Figure 3 Upper limits in the neutrino flux (90% c.l.) set by ANTARES with 2007-2010 data. The sensitivity (average upper limit) is also shown. Other limits set by different experiment are also shown for reference. An E^{-2} spectrum is assumed. (Preliminary).

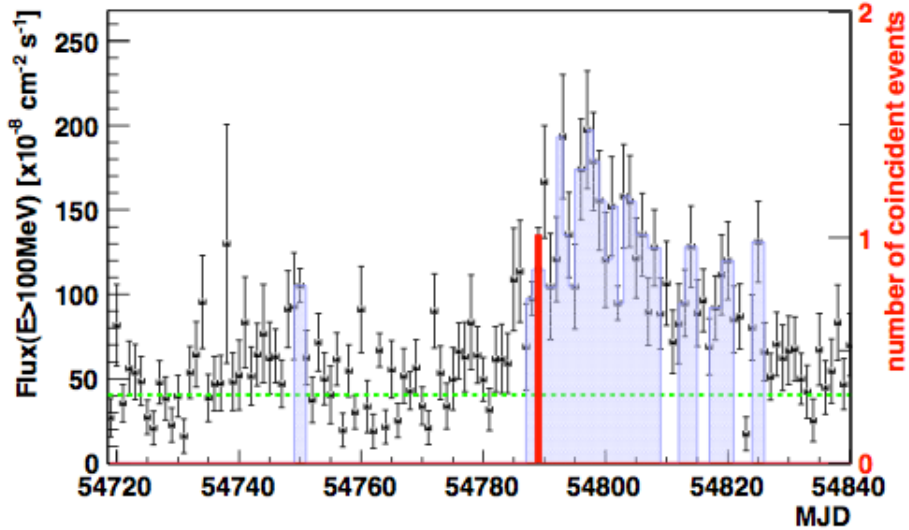


Figure 4 Gamma ray light curve of 3C279 as observed by the LAT instrument in the Fermi satellite. The red line indicates the time of the event observed by ANTARES in correlation with this flare.

4 Transient sources

For many astrophysical sources, the time information can be an additional criterion for background rejection and therefore improving the sensitivity. This is the case of catastrophic events like GRBs or flaring objects like blazars or micro-quasars. In the GRB analysis 40 bursts detected in 2007 have been investigated looking for correlations, with negative results. In the case of the blazar analysis [2], 10 flares detected in 2008 have been analyzed. In nine of them (PKS0208-512, AO0235+164, PKS1510-089, 3C273, 3C279, 3C454.3, OJ287, PKS0454-234, Wcomae and PKS2155-304), no event has been found in correlation with them. In the case of 3C279, one event is found in correlation. The corresponding p-value, taking into account the trial factor, is 0.1. Figure 4 shows the light curve for the flare of 3C279 and the time at which the neutrino event is found. Finally, in the micro-quasar analysis, 6 flares detected in 2007-2012 have been analyzed (Circinus X-1, GX339-4, H 1743-322, IGRJ17091-3624, Cygnus X-1, Cygnus X-3), with no event correlated it time.

5 Diffuse fluxes

An alternative approach in the search for cosmic sources is to integrate all the signal of the observable sky, i.e. to sum up the contributions from all the unresolved sources. The price to pay in this case is that the background cannot be rejected with the directional information and therefore is larger. However, the fact that the energy spectrum expected for cosmic sources is

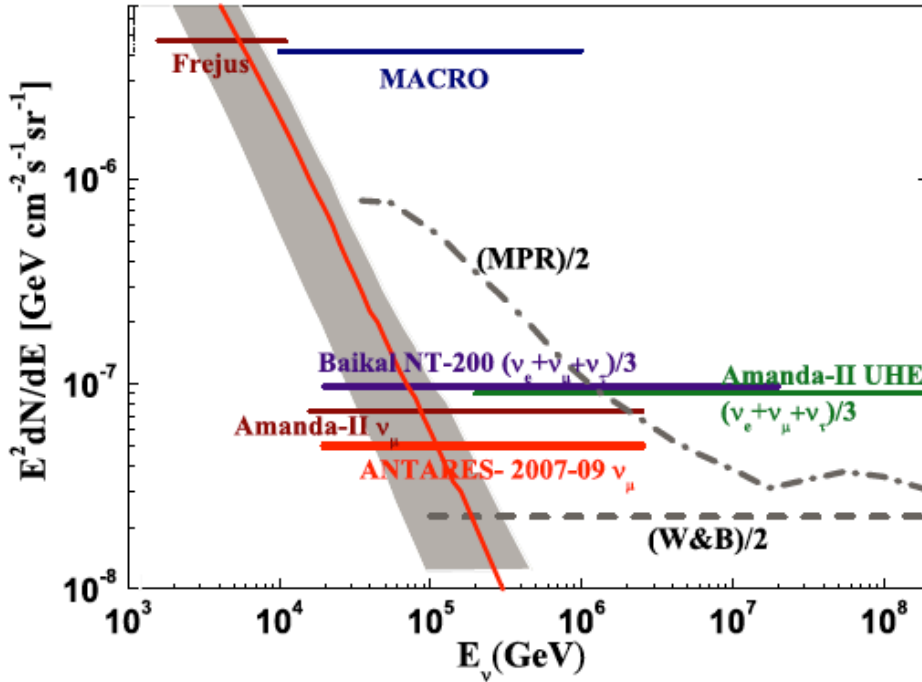


Figure 5 Upper limits at 90% c.l. for the diffuse flux contribution of neutrinos and anti-neutrinos. The grey band represent the expected atmospheric neutrino flux. Its width shows the dependence of the atmospheric flux with the zenith angle.

harder (E^{-2}) than for the atmospheric background ($E^{-3.7}$) allows for a discrimination based on some energy-depending variable. For the analysis presented here, a variable based on the number of hit repetitions in a given optical module is used. Figure 5 shows the results. Since no excess has been observed, a limit on the cosmic diffuse flux is set [9].

6 Dark matter

The search for dark matter is also one of the main goal of neutrino telescopes. They have specific advantages both when compared with other indirect searches and with direct detection experiments. If dark matter is made of WIMPs (Weakly Interacting Massive Particles), these particles would scatter in massive objects like the Sun or the Earth, lose energy and become gravitationally trapped, accumulating in the centre of the object. The Galactic Centre is also expected to have a large density of dark matter particles. After the self-annihilations of these WIMPs, high energy neutrinos are produced (either indirectly, i.e. from the secondaries produced in the WIMP self-annihilations, or directly, like in some Kaluza-Klein scenarios). The potential detection of a high energy neutrino signal from the Sun, for instance, would be a very clean signal of dark matter, since no other known astrophysical explanation would

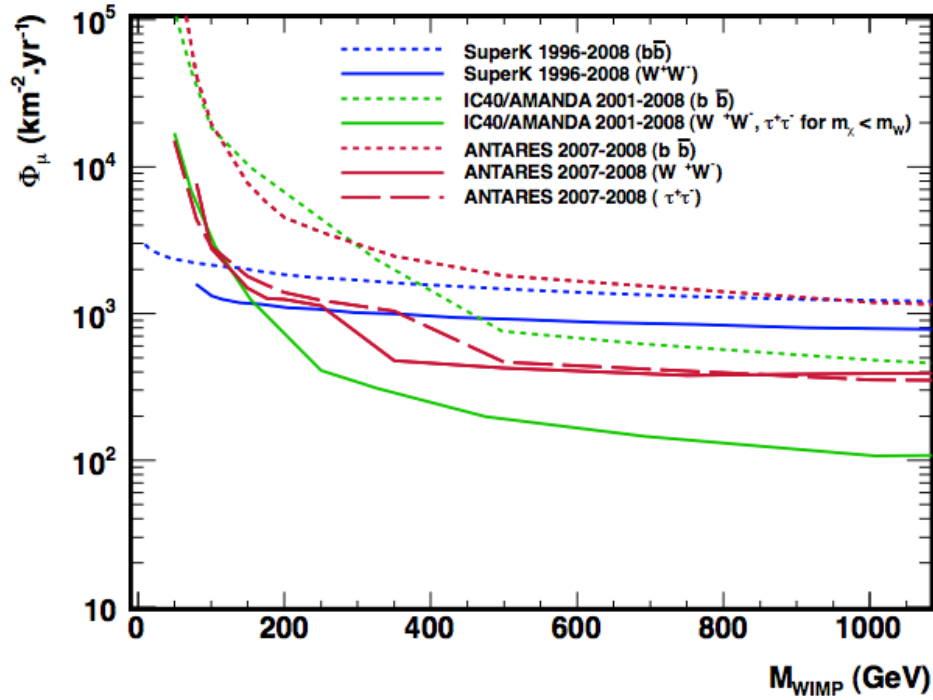


Figure 6 Limits in the neutrino flux (90% c.l.) from the Sun for several channels in the CMSSM and mUED frameworks. (Preliminary).

be able to explain it. This is not the case of observations of gamma-ray or positron excess observed by other indirect searches. Moreover, though the sensitivities for spin-independent cross sections cannot compete with those of direct search experiments (since it is proportional to the square of the atomic number of the target and in the Sun there are mostly protons and helium), this is not the case for spin-dependent cross section, where neutrino telescopes offer the best limits. The analysis made by the ANTARES collaboration is a binned search in the direction of the Sun, using data of 2007-2010 [17]. No signal has been observed, so limits in the flux are set, as shown in Fig. 6.

7 Other searches

Here we summarize other analyses performed by ANTARES:

- Gravitational waves: Several catastrophic astrophysical events are good candidates to emit both gravitational waves and neutrinos. A first analysis looking for correlations with events of VIRGO and LIGO has been done using 2007 data (where only five lines of ANTARES were installed). A second analysis, using data of 2009-2010 is ongoing [6].

- **Magnetic monopoles:** Magnetic monopoles, predicted in spontaneously broken gauge theories, would be detected in ANTARES as very bright (~ 8500 times the light output of a muon) and slowly moving events. Flux limits have been set in the range $1-9 \times 10^{-17} \text{ cm}^{-2} \text{ s}^{-1} \text{ sr}^{-1}$, a factor three better than previous searches by other experiments [3].
- **Nuclearites:** Nuclearites are stable, massive lumps of strange quark matter particles. The signature for identifying these events are slowly moving downgoing events. The data taken in 2007-2008 has allowed us to set flux limits at $1-5 \times 10^{-17} \text{ cm}^{-2} \text{ s}^{-1} \text{ sr}^{-1}$ for nuclearite masses in the range $10^{14}-10^{17} \text{ GeV}$ [15].
- **Fermi bubbles:** The so-called Fermi bubbles are two large almost spherical structures located above and below the Galactic plane, close to the Galactic Centre. Fermi-LAT has observed gamma emission with a hard and uniform spectrum. There are models which explain these structures as a consequence of hadronic acceleration. A on/off source search has found 75 events in the on-source region, whereas $90 \pm 5(\text{stat}) \pm 3(\text{sys})$ were expected from background. This excludes the fully hadronic scenario with no cut-off [14].
- **Neutrino oscillations:** Although the ANTARES detector does not aim for oscillations measurements and therefore its sensitivity cannot compete with other experiments specifically designed for such aim, it is interesting to note oscillations have been observed by ANTARES, with results compatible with the other experiments [5].

8 Conclusions

Neutrino astronomy has become a mature field and constitutes a powerful tool both in Astrophysics and Particle Physics. The ANTARES collaboration has successfully completed the construction of the first neutrino telescope in the sea. Being in the Northern Hemisphere, it can observe most of the Southern sky, including the Galactic Centre, with unsurpassed sensitivity. After five years of data taking, it has produced a rich scientific output. The physics results obtained up to now include the following searches: steady point sources, including the first map of the Southern neutrino sky; correlations with flaring sources, like micro-quasars and blazars; coincidences with GRBs; diffuse cosmic fluxes; correlation with gravitational waves; dark matter from the Sun, setting constraints in frameworks with neutrino and Kaluza-Klein particles; nuclearites, and magnetic monopoles. Even if the results of the searches has not been positive yet, the project has shown the feasibility of such a kind of detectors and therefore has paved the way to the next step, a cubic kilometer detector, KM3NeT.

Acknowledgments

The authors acknowledge the financial support of the funding agencies: Ministerio de Ciencia e Innovación (MICINN), Prometeo of Generalitat Valenciana and MultiDark, Spain

References

- [1] S. Adrián-Martínez *et al.*, ANTARES Collaboration, *Ap. J.* **743**, (2011) L14, [arXiv:1108.0292].
- [2] S. Adrián-Martínez *et al.*, ANTARES Collaboration, Accepted by *Astropart. Phys.*, [arXiv:1111.3473].
- [3] S. Adrián-Martínez *et al.*, ANTARES Collaboration, *Astropart. Phys.* **35** (2012), 634-640, [arXiv:1110.2656].
- [4] S. Adrián-Martínez *et al.*, ANTARES Collaboration, *JINST* **7** (2012), T08002, [arXiv:astro-ph/1202.3894].
- [5] S. Adrián-Martínez *et al.*, ANTARES Collaboration, *Phys. Lett.* **B714** (2012), 224-230, [arXiv:1207.3105].
- [6] S. Adrián-Martínez *et al.*, ANTARES, VIRGO and LIGO Collaboration, [arXiv:1205.3018].
- [7] S. Adrián-Martínez *et al.*, ANTARES Collaboration, Submitted to *Ap.J.*, [arXiv:1207.3105].
- [8] J. A. Aguilar *et al.*, ANTARES Collaboration, *Astropart. Phys.* **34** (2011) 539-549, [arXiv:1012.2204].
- [9] J. A. Aguilar *et al.*, ANTARES Collaboration, *Phys. Lett.* **B696**, (2011), 16-22, [arXiv:1011.3772].
- [10] J. A. Aguilar *et al.*, ANTARES Collaboration, *Nuclear Instrum. Meth. in Physics Research*, **A 656** (2011), 11-38, [arXiv:1104.1607v1].
- [11] W. Bednarek *et al.*, *New Astron. Rev.* **49** (2005) 1, [arXiv:astro-ph/0404534].
- [12] E. G. Berezhko, H. J. Völk, *Astronomy and Astrophysics*, **492**, 3 (2008), 695-701, [arXiv:0810.0988v2].
- [13] F. Halzen, D. Hooper, *Rep. Prog. Phys.* **65** (2002) 1025, [arXiv:astro-ph/0204527].
- [14] V. Kulikovskiy, Neutrino 2012 Conference, Kyoto 2012.
- [15] G. Pavalas, Proc. of the CSSP10 conference, Sinaia (2010), [arXiv:1010.2071v1].
- [16] F. W. Stecker, *Phys. Rev. D* **72** (2005) 107301, [arXiv: astro-ph/0510537].
- [17] J.D. Zornoza, *Nucl. Instrum. Meth. A* **692** (2012) 123-126, [arXiv:1204.5066].